2021 NDIA GROUND VEHICLE SYSTEMS ENGINEERING AND TECHNOLOGY SYMPOSIUM
MODELING SIMULATION & SOFTWARE (MS2) TECHNICAL SESSION
AUGUST 10-12, 2021 - NOVI, MICHIGAN

INVERSE DYNAMICS APPROACH TO ESTABLISH MOBILITY MARGINS

Jesse Paldan[1], Vladimir Vantsevich, PhD[1], David Gorsich, PhD[2], Paramsothy Jayakumar, PhD[2], Lee Moradi, PhD[1]

[1]The University of Alabama at Birmingham
[2] U.S. Army DEVCOM Ground Vehicle Systems Center

ABSTRACT

An inverse dynamics approach is applied to assess the relationship and establish an adjustable balance between acceleration performance, slip energy efficiency, and mobility margins of a wheel of a vehicle with four wheels individually-driven by electric DC motors. The time history of the reference wheel torques are recovered which would enable the motion at the desired linear velocity. Target velocity profiles are applied which provide different rates of acceleration. The profiles are simulated in stochastic terrain conditions which represent continuously changing, uncertain terrain characteristics with various quality of rolling resistance and peak friction coefficient. A wheel mobility margin is determined to track how close a driving wheel is to immobilization. When moving in drastically changing stochastic terrain conditions, boundaries are adjusted to accommodate changes in the resistance to motion in order to guarantee the motion while not exceeding limits which would cause excessive tire slippage. The mathematical models were developed in a way to facilitate their applicability for autonomous vehicles.

Citation: J. Paldan, V. Vantsevich, D. Gorsich, P. Jayakumar, L. Moradi, “Inverse Dynamics Approach to Establish Mobility Margins”, In *Proceedings of the Ground Vehicle Systems Engineering and Technology Symposium* (GVSETS), NDIA, Novi, MI, Aug. 10-11, 2021.

1. INTRODUCTION

The mobility and the energy efficiency of vehicles are aspects that have been studied using different approaches. Approaches to assess mobility include terramechanics and vehicle dynamics-based methods. To evaluate mobility with terramechanics methods, a large amount of experimental data is needed; data compiled from field and laboratory tests is used to authenticate mobility prediction models for evaluating tractive performance of off-road vehicle motion [1, 2]. Sophisticated computer models of soil elements have high computational complexity that limit real-time application and work is being done to improve the efficiency of models to bring down the computation time [3].

From the vehicle dynamics side of mobility, the use of individual electric motors has been studied for application to traction, slip, and speed control functions in conditions including off-road motion, icy roads, and hill climbing [4]. To bridge the terramechanics and vehicle dynamics aspects of mobility, applications of sensors are applied to link measurements of soil information to wheel parameters and forces [5]. Another goal of research is the improvement of energy efficiency through application of wheel control algorithms [6].

Mobility and energy efficiency were never considered together to establish reasonable balance and limits for improving and sacrificing one for another. They are instead considered separately or as the same problem. In this paper, mobility and energy efficiency are considered as separate aspects and an approach considered to evaluate and make tradeoffs between them.

Terrain mobility of a vehicle is its overall capability to move from place to place while retaining its ability to perform its primary task/mission. The ability to perform the task can be evaluated by the vehicle's ability to meet a desired velocity and its changes, i.e., an acceleration profile, while the capability to move is determined by the mobility margins. A mobility margin is defined as the relation of the current state of the vehicle or wheel to its immobilization state. When the vehicle has sufficient mobility margins, it still possesses the ability to increase velocity without becoming immobilized. Drops in the mobility margins are accompanied obviously by increases in tire slippage. Autonomous vehicle control systems, when being designed for off-road use, require the ability to evaluate the mobility margins.

Energy efficiency is another crucial operational property that an autonomous electric vehicle should be able to self-assess and control [7, 8]. Tire slippage, which is paramount for mobility assessment, also impacts energy efficiency as power losses due to slippage. Thus, studying the impact the tire slippage on mobility (in terms of performance and margins) and energy efficiency becomes important for establishing reasonable balance that can be used in on-board assessment and controls of autonomous vehicles.

Slip power is the power lost in deflecting the tire and the soil in the longitudinal direction, resulting in loss of the linear velocity of the wheel V_δ given by the expression [9]

$$V_\delta = V_t - V_x \tag{1}$$

where V_x is the actual linear velocity and V_t is the theoretical linear velocity without slip.

The rolling radius r_w of a wheel with an elastic tire is the radius of a hypothetical rigid wheel that has the same linear velocity V_x as the real pneumatic wheel [9]. Rolling radius r_w is the non-physically measurable radius which gives velocity V_x when multiplied by the wheel's angular velocity ω_w:

$$V_x = r_w \omega_w \tag{2}$$

The theoretical linear velocity V_t is determined using the rolling radius in the driven mode r_w^0 (wheel is driven with zero applied torque) as the reference rolling radius of the tire without slip [9].

$$V_t = r_w^0 \omega_w \tag{3}$$

Equation (1), after substituting the components of V_x and V_t and multiplying by the wheel circumferential force F_x, gives the slip power:

$$P_\delta = F_x \omega_w (r_w^0 - r_w) \tag{4}$$

In this paper, a method is devised to assess mobility margins of a wheel of 4x4 vehicle with individually-driven wheels. The overall goal of the task in simulation is to aim for fast-enough-acceleration to a target linear velocity while maintaining tire mobility margins at high levels. The dynamically varying balance between acceleration performance and energy efficiency is established for different levels of the mobility margins. For this purpose, an inverse dynamics approach is developed in the paper to involve the calculation of wheel forces or torques that correspond to given target kinematic parameters of the vehicle.

2. INVERSE DYNAMICS MODEL

In the inverse dynamics approach, the reference wheel torque can be obtained from a given reference velocity $V_x = f(t)$. Forces, torques, and kinematic parameters are shown in figure 1 for a single-wheel module.

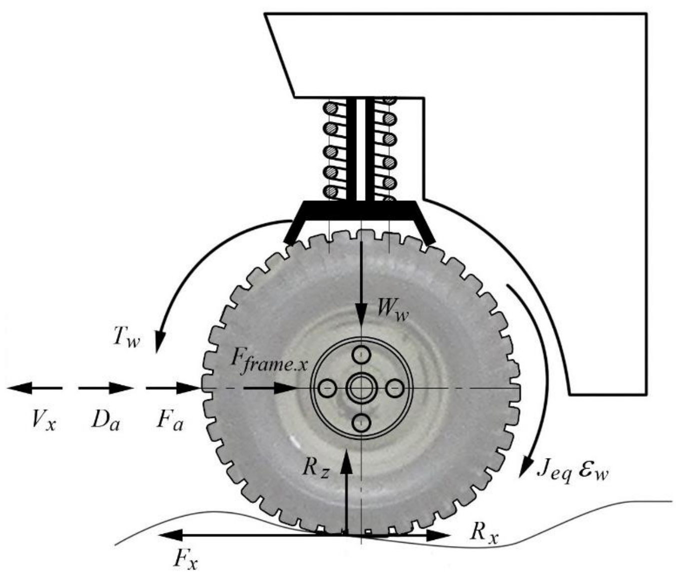

Figure 1: Wheel in non-stationary motion

The reference torque T_w is

$$T_w = F_x r_w^0 + J_{eq}\varepsilon_w + B_{eq}\omega_w \quad (5)$$

where F_x is the wheel circumferential force, J_{eq} and B_{eq} are the rotational inertia and damping of the wheel and driveline reduced to the wheel axis, and ε_w is the angular acceleration. An empirical formula (6) relates r_w^0 to the tire inflation pressure p_w and the normal reaction R_z [10].

$$r_w^0 = r\frac{rp_w + \upsilon_1 R_z}{rp_w + \upsilon_2 R_z} \quad (6)$$

υ_1 and υ_2 are empirical coefficients determined from experimental data of a tire. The circumferential force is the force at the tire patch developed by the wheel torque which provides the traction. For the reference velocity profile, F_x is

$$F_x = R_x + F_{frame.x} + D_a + F_a \quad (7)$$

where R_x is the stochastic rolling resistance modeled with the method described in [11], $F_{frame.x}$ is the force from the vehicle frame/drawbar pull, D_a is a part of the vehicle air drag computed based on the given velocity profile, and F_a is the acceleration force obtained by multiplying the wheel module mass by the reference linear acceleration. Thus, equation (7) represents the inverse dynamics approach, in which the wheel circumferential force is computed for given kinematic parameters.

Circumferential force is linked to the tire slippage; the following nonlinear equation is used to calculate tire slippage s_δ from the circumferential force [9]:

$$F_x = \mu_{px} R_z (1 - e^{-ks_\delta}) \quad (8)$$

μ_{px} is the peak friction coefficient and k is an empirical factor obtained from approximation of experimental data.

The meaning of the peak friction coefficient can be understood from figure 2 and equations (9-10). When F_x is normalized by the normal reaction R_z, the result is the current friction coefficient μ_x:

$$\mu_x = \mu_{px}(1 - e^{-ks_\delta}) \quad (9)$$

μ_x represents the percentage of the normal reaction R_z that is utilized in generating the circumferential force $F_x$needed for motion under the given conditions [9]:

$$\mu_x = \frac{F_x}{R_z} \quad (10)$$

Figure 2 is a plot of the normalized slippage curve from equation (9).

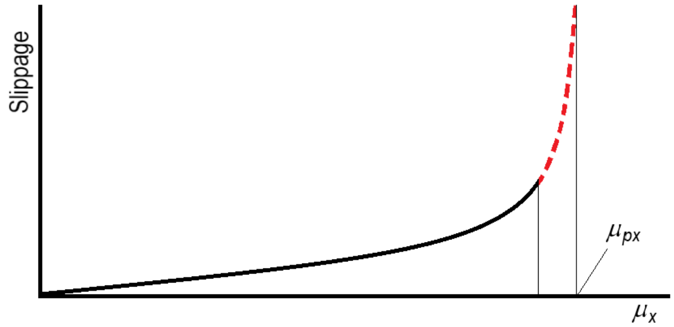

Figure 2: Stochastic current and peak friction coefficients μ_x and μ_{px}

μ_x asymptotically approaches μ_{px}. The peak friction coefficient determines the maximum possible circumferential force under the current traction condition; μ_{px} is not a constant but a stochastic variable [11]. If the values taken by μ_x during the wheel motion overlap the range in stochastic values of μ_{px}, the wheel is at risk of immobilization. The stochastic peak friction coefficient can change drastically when a wheel moves from one terrain condition to another. As seen in the dashed line section of the curve in figure 2, when μ_x is getting close to μ_{px}, the slippage starts to increase rapidly and the wheel is very close to becoming immobilized since slippage is drastically increasing to its higher values.

As an estimate of the wheel mobility, the Wheel Mobility Index (WMI) is used [12].

$$WMI = 1 - \frac{F_x}{F_x^{max}} = 1 - \frac{F_x}{\mu_{px} R_z} \qquad (11)$$

WMI is the remaining capacity for mobility (mobility margin) obtained by comparing the current f F_x to the maximum $F_x^{max} = \mu_{px} R_z$ from the traction-slip curve in equation (8). For non-steady motion, the WMI is re-written in terms of wheel torque with the inertia and damping terms included.

$$WMI = 1 - \frac{T_w - J_{eq}\varepsilon_w - B_{eq}\omega_w}{r_w^0 \mu_{px} R_z} \qquad (12)$$

The wheel maintains a margin of mobility when its current friction coefficient is less than the maximum, meaning the wheel still has a margin to increase acceleration or overcome additional resistance without leading to immobilization.

The wheel's angular velocity may be obtained by dividing linear velocity, which is assigned in the velocity profile, by the tire rolling radius in the driving mode at a non-zero torque.

$$\omega_w = \frac{V_x}{r_w} \qquad (13)$$

The tire rolling radius in the driving mode, r_w, accounts for the decrease in velocity due to tire slippage from the theoretical velocity V_t without slip to velocity V_x:

$$s_\delta = \frac{V_t - V_x}{V_t} = \frac{\omega_w r_w^0 - \omega_w r_w}{\omega_w r_w^0} = 1 - \frac{r_w}{r_w^0} \qquad (14)$$

Solving for r_w allows the rolling radius of a driving wheel to be calculated from the slippage and rolling radius in the driven mode r_w^0.

$$r_w = r_w^0(1 - s_\delta) \qquad (15)$$

3. INVERSE DYNAMICS SIMULATION RESULTS

A simulation model was created of individually-driven wheel module of a 4x4 vehicle with four wheels individually-driven by electric DC motors. The wheel module has a sprung mass of 1649 kg and unpsrung mass of 236 kg. A set of three velocity profiles was generated for an acceleration from 0 to 40 mph in 30 seconds. Shown in figure 3, the profiles 1-3 have different accelerations to the target speed; the maximum acceleration is given in Table 1.

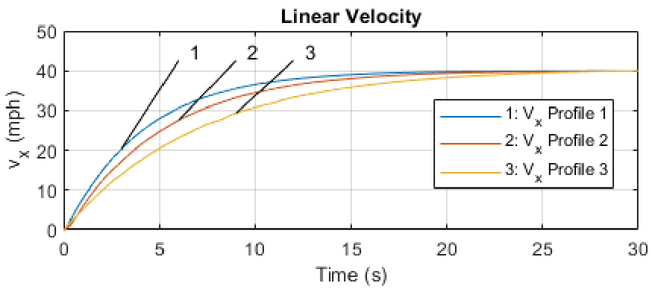

Figure 3: Reference velocity profiles

Table 1: Maximum acceleration in m/sec^2

Profile	1	2	3
Max Acceleration	4.7236	3.3499	2.7260

A terrain input was generated using the process detailed in [11]. The stochastically-varying ground height produces stochastic variance in the peak friction coefficient, used in equation (8), and the rolling resistance coefficient. The rolling resistance coefficient, when multiplied by the normal reaction, determines the magnitude of the rolling resistance force R_x. Two terrains were generated, a meadow (off-road condition) and asphalt road (figure 4).

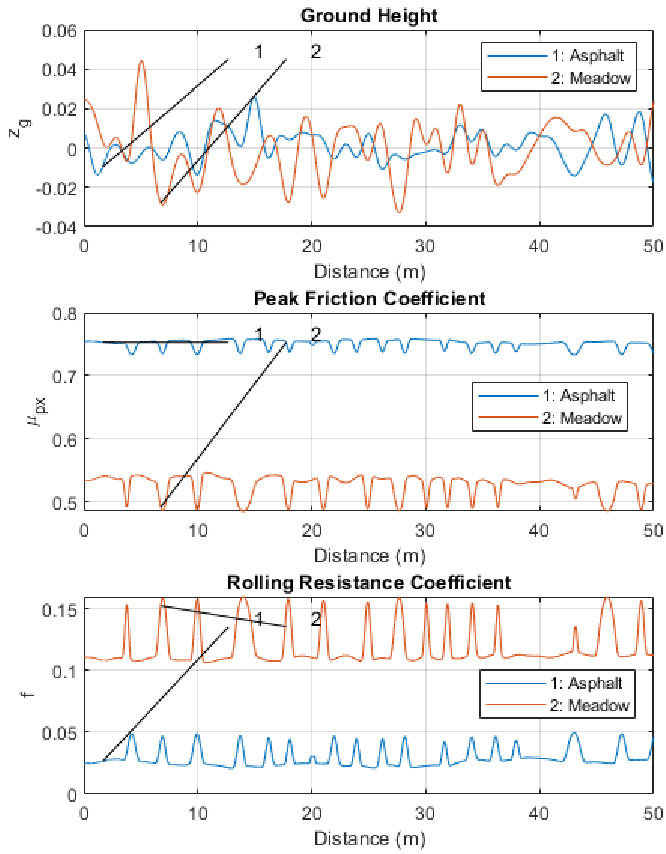

Figure 4: Stochastic terrain conditions

Figure 5 shows the required wheel torques for the wheel to make each of the three velocity profiles given in figure 4 on the two terrains.

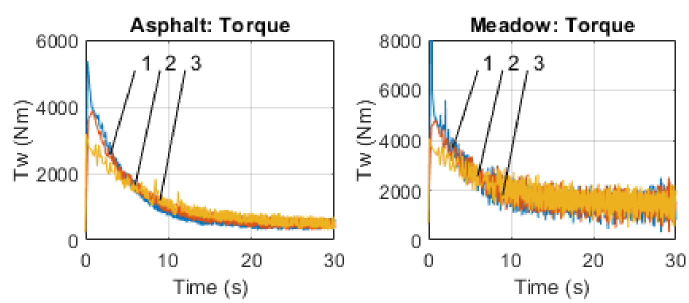

Figure 5: Wheel torques

Figure 6 shows the wheel tire slippage ratios. The higher torques of profile 1 allow the wheel to reach higher acceleration, but also produce higher circumferential forces and tire slippage.

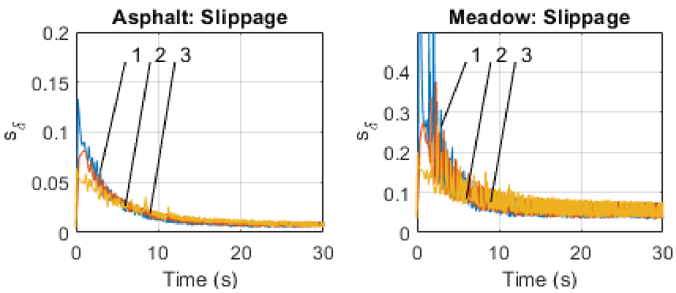

Figure 6: Tire slippage ratios

Figure 7 is the power losses due to the tire slippage and figure 8 shows the driving mode rolling radius, which decreases with increases in slippage.

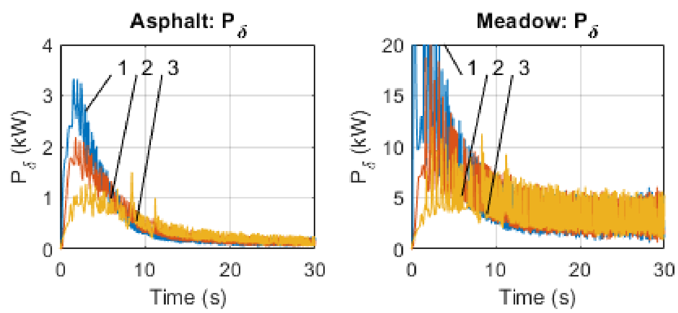

Figure 7: Slip power losses

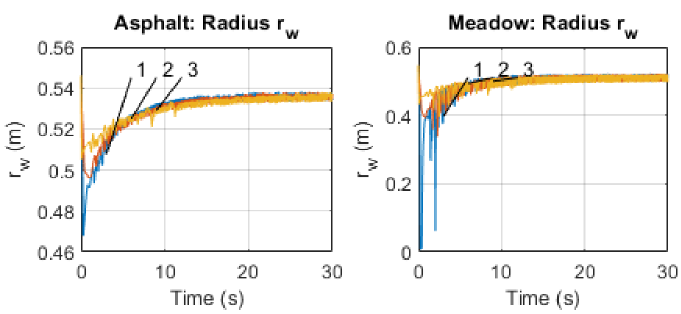

Figure 8: Driving mode rolling radius

The mobility margins are shown by the WMI in figure 9. With the first profile, on meadow terrain the WMI drops critically low at the beginning of the motions, which correspond to the drops in rolling radius and excessive slip power losses in figures 7 and 8.

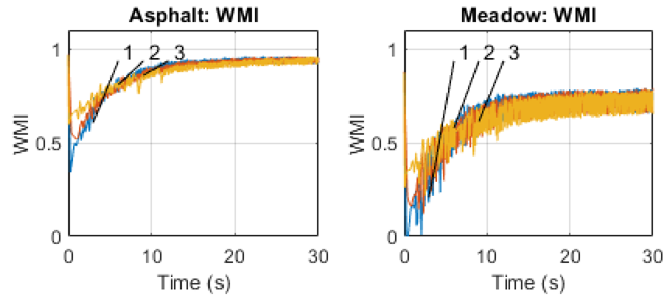

Figure 9: Wheel mobility index

Figures 10 and 11 plot the relation between the speed, mobility margin, and slip power losses to more clearly show the change in mobility performance and power losses when selecting profiles 1-3.

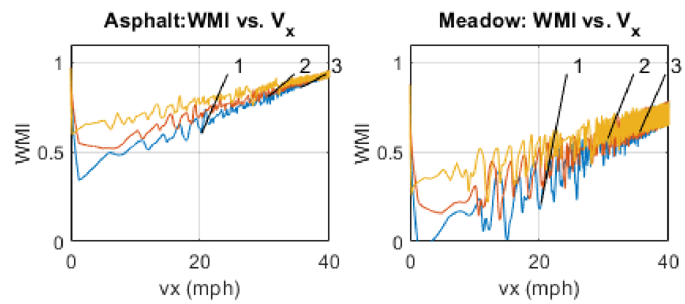

Figure 10: WMI vs. linear speed

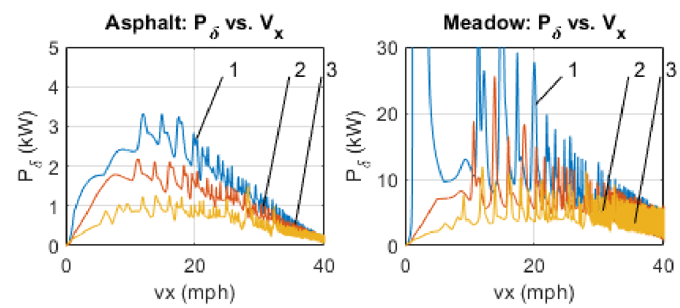

Figure 11: Slip power losses vs. linear speed

For the meadow terrain, a reduction in the torque or one of the less aggressive velocity profiles is needed to ensure mobility performance and avoid excessive power losses.

Figure 12 shows the mobility margin plotted against the torque.

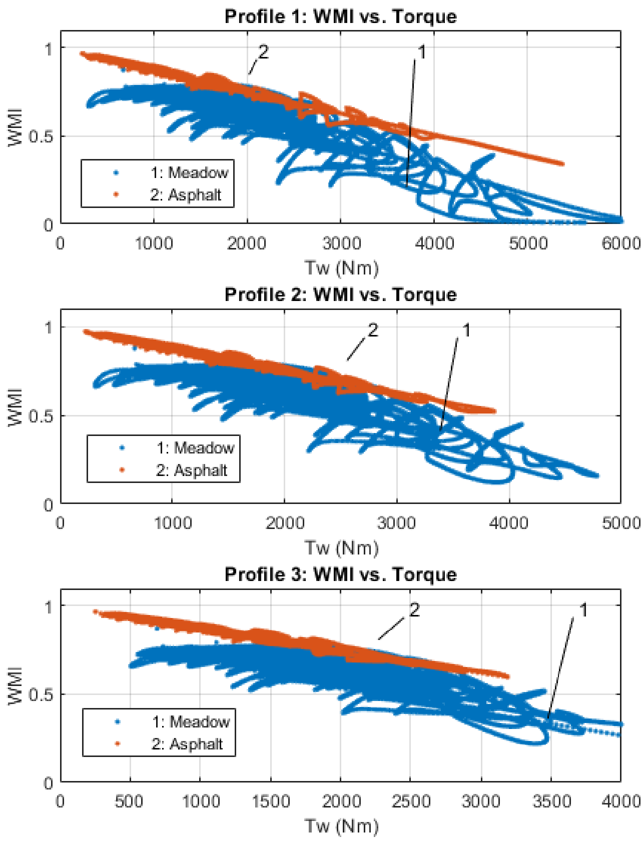

Figure 12: Relationship between torque and mobility index

The distribution of data points demonstrates an inverse relationship between the wheel torque and mobility margins, in which all three profiles follow the same pattern. In figure 13, a linear function was fitted to the points for both terrains.

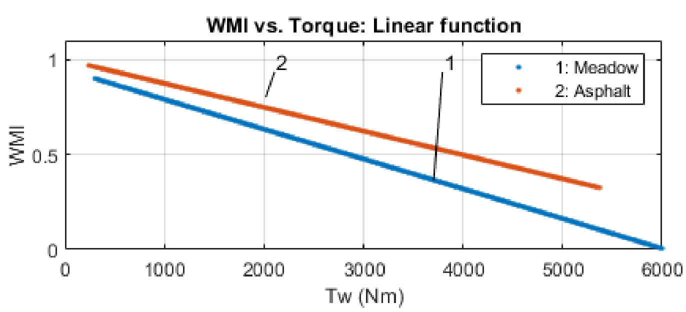

Figure 13: Linear function approximating the relationship between torque and mobility index

Figure 13 allows the determination of mobility margins-based torque boundaries. A limit on the torque may be selected which corresponds to a chosen mobility margin.

To evaluate the acceleration performance of the wheel along with the energy efficiency when different margins are selected, a series of simulations were run using wheel torques selected to match a range of WMI boundaries from figure 13. The results are summarized in figures 14 and 15. The curves show a characteristic of the time to accelerate up to 40 mph plotted alongside a characteristic of the work done on tire slippage, obtained by summing the total slip power losses over the period of motion. The characteristics of the time and work are obtained by normalizing by their minimum and maximum values.

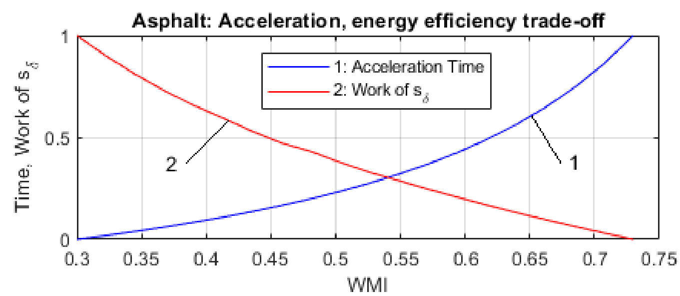

Figure 14: Tradeoff between acceleration time and energy losses (asphalt)

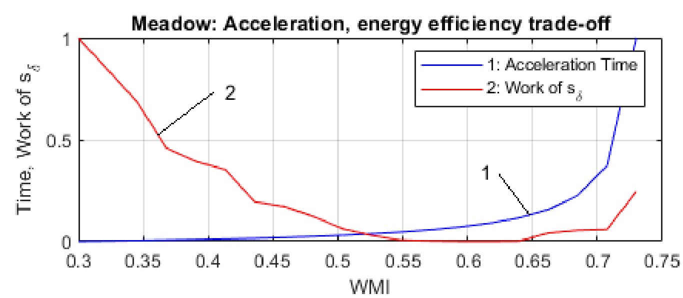

Figure 15: Tradeoff between acceleration time and energy losses (meadow)

The graphs allow analysis of the tradeoffs between performance, characterized by the acceleration time, and energy efficiency, characterized by the work when selecting a particular mobility margin. A lower acceleration time is achieved by selecting a lower boundary from the left side of the chart. As the boundary is increased moving to the right side of the chart, the work decreases while the acceleration time increases. On the meadow terrain, a very strict boundary above 0.7 results in a degradation in efficiency as more power is expended across the long acceleration time than is saved by the lessened acceleration. A more efficient result is achieved by selecting a balanced boundary at the intersection of the two curves.

When the vehicle moves from one terrain to another (figure 16), friction and rolling resistance characteristics can change quickly, requiring quick adaptation.

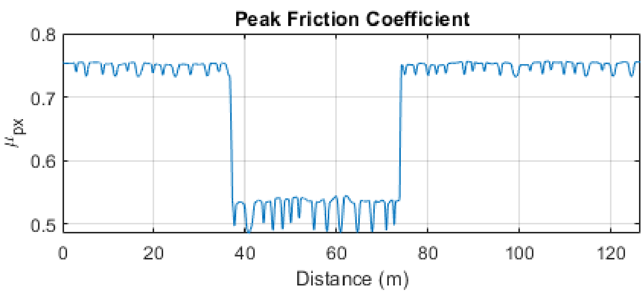

Figure 16: Changing terrain profile

In figure 17, a wheel torque was selected to keep an average WMI of 60%. When the wheel encounters the drop in the peak friction coefficient, the slippage increases with a corresponding drop in WMI.

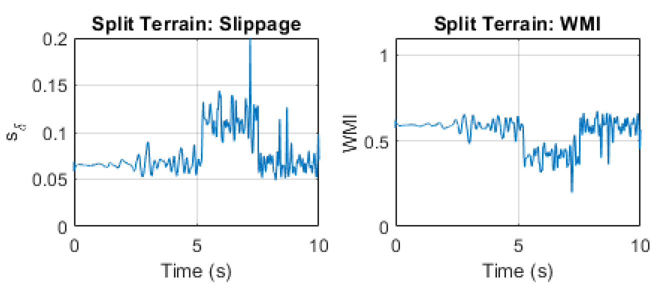

Figure 17: Slippage and WMI on changing terrain, constant torque boundary

In figure 18, the torque boundary is changed upon crossing the terrain boundary, resulting in the linear velocity shown.

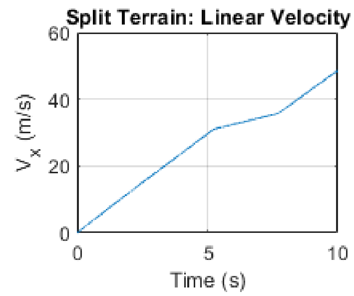

Figure 18: Linear velocity on changing terrain

The torque is dropped to maintain the margin of 60%, allowing the wheel to maintain the WMI at a consistent level and avoid increase in the slippage.

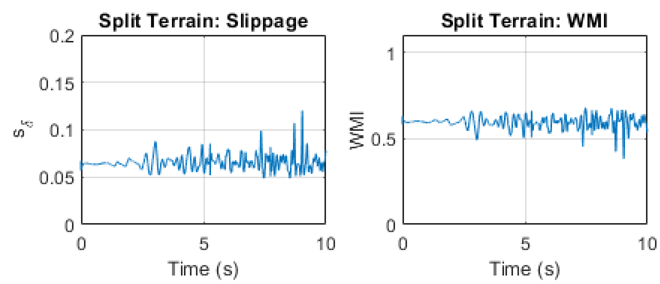

Figure 19: Slippage and WMI on changing terrain, changed torque boundary

Results in figures 14-19 are not using the same velocity profiles, but were built based on the torque-WMI relationship derived from the original velocity profiles. As shown by figure 12, the function relating the torque and WMI can be obtained for any given profiles of the original velocities, which can be assigned based on the tasks of the vehicle.

4. CONCLUSION

An inverse dynamics problem was formulated to establish a dynamic balance between acceleration performance and energy efficiency while maintaining the Wheel Mobility Index. The problem was solved by recovering the wheel torque that maintains a given velocity profile. Simulation results of a wheel moving with the recovered reference torques were analyzed to determine mobility performance and power losses of the wheel in stochastic terrain conditions. The wheel mobility index was used to determine boundaries on the torque which keep mobility at a desired margin. The tradeoffs between acceleration performance and energy efficiency were analyzed when assigning a particular mobility margin. The application of the boundaries provides a guideline for balancing characteristics for mobility, performance, and efficiency of autonomous vehicles.

5. REFERENCES

[1] F. Vahedifard, J. Robinson, G. Mason, I. Howard, and J. Priddy, "Mobility algorithm evaluation using a consolidated database developed for wheeled vehicles operating on dry sands," Journal of Terramechanics, Volume 63, 2016.

[2] C. Senatore, and C. Sandu, "Torque distribution influence on tractive efficiency and mobility of off-road wheeled vehicles, Journal of Terramechanics," Volume 48, Issue 5, 2011.

[3] P. Yang, M. Zang, H. Zeng, and X. Guo, "The interactions between an off-road tire and granular terrain: GPU-based DEM-FEM simulation and experimental validation," International Journal of Mechanical Sciences, Volume 179, 2020.

[4] D. Savitski, D. Schleinin, V. Ivanov, K. Augsburg, E. Jimenez, R. He, C. Sandu, and P. Barber, "Improvement of traction performance and off-road mobility for a vehicle with four individual electric motors: Driving over icy road," Journal of Terramechanics, Volume 69, 2017.

[5] H. Tsubaki, G. Ishigami, "Experimental study on wheel-soil interaction mechanics using in-wheel sensor and particle image velocimetry Part I: Analysis and modeling of normal stress of lightweight wheeled vehicles," Journal of Terramechanics, 2021.

[6] M. Yacoub, D. Necsulescu, and J. Sasiadek, "Energy Consumption Optimization for Mobile Robots Motion Using Predictive Control," Journal of Intelligent & Robotic Systems 83, 2016.

[7] U.S. Army Robotic and Autonomous Systems Strategy (RAS), 2017.

[10] J. Palmer, G. Hamilton, and M. Smith, "A Strategy for Intelligent Platform Power Management Within Ground Combat Vehicles," NDIA Ground Vehicle Systems Engineering and Technology Symposium, 2012.

[9] A. Andreev, V. Kabanau, and V. Vantsevich, "Driveline of Ground Vehicles: Theory and Design," Taylor and Francis Group/CRC Press, 2010.

[10] V. Petrushov, S. Shuklin, and V. Moskovkin, "Rolling Resistance of Automobiles and Trucks," Mashinostroenie Publishing House, Moscow, Russia, 1975 (in Russian).

[11] J. Gray, V. Vantsevich, A. Opeiko, and G. Hudas, "A Method for Unmanned Ground Wheeled Vehicle Mobility Estimation in Stochastic Terrain Conditions," Proc. of the 7th Americas Regional Conference of the ISTVS, 2103.

[12] J. Gray, V. Vantsevich, and J. Overholt, "Indices and Computational Strategy for Unmanned Ground Wheeled Vehicle Mobility Estimation and Enhancement," ASME International Design Engineering Technical Conferences and Computers and Information in Engineering Conference, 2013.